INVITED PAPER

Modeling and Simulation of Electric and Hybrid Vehicles

Tools that can model embedded software as well as components, and can automate the details of electric and hybrid vehicle design, need to be developed.

By David Wenzhong Gao, *Senior Member IEEE*, Chris Mi, *Senior Member IEEE*, and Ali Emadi, *Senior Member IEEE*

ABSTRACT | This paper discusses the need for modeling and simulation of electric and hybrid vehicles. Different modeling methods such as physics-based Resistive Companion Form technique and Bond Graph method are presented with powertrain component and system modeling examples. The modeling and simulation capabilities of existing tools such as Powertrain System Analysis Toolkit (PSAT), ADvanced VehIcle SimulatOR (ADVISOR), PSIM, and Virtual Test Bed are demonstrated through application examples. Since power electronics is indispensable in hybrid vehicles, the issue of numerical oscillations in dynamic simulations involving power electronics is briefly addressed.

KEYWORDS | ADVISOR; bond graph; electric vehicles; hybrid electric vehicle (HEV); hybrid vehicles; modeling and simulation; physics-based modeling; Powertrain System Analysis Toolkit (PSAT); PSIM; saber; simplorer; Virtual Test Bed (VTB)

I. INTRODUCTION

Compared to conventional vehicles, there are more electrical components used in electric, hybrid, and fuel cell vehicles, such as electric machines, power electronics, electronic continuously variable transmissions (CVT), and embedded powertrain controllers [1], [2]. Advanced energy storage devices and energy converters, such as Li-ion batteries, ultracapacitors, and fuel cells, are introduced in the next generation powertrains. In addition to these electrification components or subsystems, conventional internal combustion engines (ICE) and mechanical and hydraulic systems may still be present. The dynamic interactions among various components and the multidisciplinary nature make it difficult to analyze a newly designed hybrid electric vehicle (HEV). Each of the design parameters must be carefully chosen for better fuel economy, enhanced safety, exceptional drivability, and a competitive dynamic performance—all at a price acceptable to the consumer market. Prototyping and testing each design combination is cumbersome, expensive, and time consuming. Modeling and simulation are indispensable for concept evaluation, prototyping, and analysis of HEVs. This is particularly true when novel hybrid powertrain configurations and controllers are developed.

Furthermore, the complexity of new powertrain designs and dependence on embedded software is a cause of concern to automotive research and development efforts. This results in an increasing difficulty in predicting interactions among various vehicle components and systems. A modeling environment that can model not only components but also embedded software, such as the Electronic Throttle Controller (ETC) software, is needed. Effective diagnosis also presents a challenge. Modeling can play an important role in the diagnostics of the operating components. For example, running an embedded fuel cell model and comparing the actual fuel cell operating variables with those obtained from the model can help fault diagnosis of fuel cells.

A face-off with modeling and simulation tools in the electronics industry has demonstrated that similar tools in the automotive domain still lack the power, sophistication, and automation required by the electronics designers [3]. Advances in electronic design tools have validated Moore's law (as applied to the complexity of integrated circuits) and have helped achieve amazing standards in computing power while simultaneously decreasing costs. For designers of automotive systems to duplicate and manage similar levels of complexity, design tools that automate the

Manuscript received July 8, 2006; revised November 2, 2006.
D. W. Gao is with Center of Energy Systems Research, Department of Electrical and Computer Engineering, Tennessee Technological University, Cookeville, TN 38501 USA (e-mail: wgao@tntech.edu).
C. Mi is with the Department of Electrical and Computer Engineering, University of Michigan, Dearborn, MI 48128 USA (e-mail: mi@ieee.org).
A. Emadi is with the Department of Electrical and Computer Engineering, Illinois Institute of Technology, Chicago, IL 60616-3793 USA (e-mail: emadi@iit.edu).
Digital Object Identifier: 10.1109/JPROC.2006.890127

low-level details of the design process need to be developed [3], [4].

Depending on the level of details of how each component is modeled, the vehicle model may be steady-state, quasi-steady, or dynamic [5]–[15]. For example, the ADVISOR [5], [6] model can be categorized as a steady-state model, the PSAT [7] model as quasi-steady one, and PSIM [8] and Virtual Test Bed (VTB) [9] models as dynamic. On the other hand, depending on the direction of calculation, vehicle models can be classified as forward-looking models or backward facing models [5]. In a forward-looking model, vehicle speed is controlled to follow a driving cycle during the analysis of fuel economy, thus facilitating controller development.

The main advantage of employing a steady-state model or quasi-steady model is fast computation, while the disadvantage is inaccuracy for dynamic simulation. On the contrary, physics-based models can facilitate high fidelity dynamic simulations for the vehicle system at different time scales. This kind of dynamic model should be useful for developing an effective powertrain control strategy [10]. The models are tied closely to the underlying physics through a link such as a lumped-coefficient differential equation or some digital equivalent model.

This paper addresses different modeling and simulation methods for electric and hybrid vehicles. The rest of the paper is organized as follows: Section II reviews the fundamentals of vehicle system modeling. Sections III and IV provide an overview of existing vehicle modeling tools, ADVISOR and PSAT, with application examples, i.e., using ADVISOR to study hybrid battery/ultracapacitor energy storage system and using PSAT to optimize a parallel powertrain design, etc. Section V looks at physics-based dynamic modeling, introducing the Resistive Companion Form (RCF) modeling method with modeling examples of a dc machine, a dc/dc boost power converter, and vehicle dynamics including wheel slip model. Section VI looks at bond graphs and other modeling tools such as PSIM, Simplorer, V-ELPH [12], Saber, and Modelica for hybrid powertrain modeling. Section VII addresses the issue and mitigation methods of numerical oscillations for dynamic simulation involving power electronics. Finally, conclusions are given in Section VIII.

II. FUNDAMENTALS OF VEHICLE SYSTEMS MODELING

It is important to define the common terms used in modeling. The following definitions are based on the text by Dr. P. Fritzson of the Linköping University, Sweden [16], and are related to HEV modeling.

1) System: The object or objects we wish to study. In the context of this paper, the system will be an electric or HEV.
2) Experiment: The act of obtaining information from a controllable and observable system by intelligently varying system inputs and observing system outputs.
3) Model: A surrogate for a real system upon which "experiments" can be conducted to gain insight about the real system. The types of experiments that can be validly applied to a given model are typically limited. Thus, different models are typically required for the same target system to conduct all of the experiments one wishes to conduct. Although there are various types of models (e.g., scale models used in wind tunnels), in this paper, we will mainly discuss about physics-based mathematical models.
4) Simulation: An experiment performed on a model.
5) Modeling: The act of creating a model that sufficiently represents a target system for the purpose of simulating that model with specific predetermined experiments.
6) Simulator: A computer program capable of performing a simulation. These programs often include functionality for the construction of models and can often be used in conjunction with advanced statistical engines to run trade studies, design of experiments, Monte Carlo routines, and other routines for robust design.

Vehicle system modeling is conducted over various areas of interest to answer vastly different questions (i.e., different experiments). Traditional areas include modeling for the analysis of vibration, handling, and noise (NVH), modeling of vehicle performance (e.g., acceleration, gradeability, and maximum cruising speed); modeling for the prediction, evaluation, and optimization of fuel economy; modeling for safety, stability, and crash worthiness; modeling of vehicle controls; modeling for structural integrity; modeling to facilitate component testing and validation; modeling for preliminary concept design/design exploration; modeling for cost and packaging; and modeling for the prediction of emissions.

There are various types of mathematical models and simulators available to perform vehicle system simulations. For example, some simulators can be used to construct models that use macro statistics from duty cycles and cycle-averaged efficiencies of components for near instantaneous prediction of fuel consumption and performance, whereas other simulators perform detailed subsecond transient simulations for more detailed experiments. There is also typically a tradeoff in the vehicle modeling between the amount of engineering assumptions the modeler has to make and the amount of time required to set up and construct a model. A simple high-level model can estimate fuel consumption using the engineer's knowledge of "typical" cycle-averaged component efficiencies. A more detailed model would actually simulate each of the components over time and mathematically determine cycle-averaged efficiencies. In addition to the

assumption/specificity tradeoff, there is also a tradeoff between model detail and run time. In general, the more detailed results one needs, the longer the total time for model setup, simulation, and interpretation of results.

Detailed vehicle system models typically contain a mix of empirical data, engineering assumptions, and physics-based algorithms. Good simulators provide a large variety of vehicle components along with data sets to populate those components. The components can then be connected together as the user desires to create a working vehicle powertrain, body, and chassis. Connections between components mathematically transmit effort and flow (e.g., torque and speed or voltage and current) during a simulation.

Depending upon the degree of details desired, there are various models available such as steady-state spreadsheet models, transient power-flow models, and transient effort-flow models (effort/flow refers to the combinations of torque/angular speed, voltage/current, force/linear speed, etc.).

The transient vehicle system models can be divided into two categories based on the direction of calculation. Models that start with the tractive effort required at the wheels and "work backward" towards the engine are called "backward facing models." Models that start from the engine and work in transmitted and reflected torque are called "forward facing models." So-called noncausal models allow for forward or backward operation depending on the experiment being performed. Backward facing models are typically much faster than forward-facing models in terms of simulation time. Forward-facing models better represent real system setup and are preferred where controls development and hardware-in-the-loop will be employed. Forward models must typically use some kind of "driver model" such as a PID controller to match a target duty cycle. Some "hybrid" models include both concepts.

In addition, vehicle systems models may interact with any number of more detailed models such as structural analysis models, vibrational models, thermal models, etc.

Driven by the need for fast simulation times, complex components such as engines and motors are typically simulated using "lookup maps" of energy consumption versus shaft torque and angular speed. Once the average torque and angular shaft speed for a given time-step are determined, an interpolation on empirical data is performed to determine the component's energy consumption rate.

There have been extensive studies in the modeling and simulation of hybrid and electric vehicles [4]–[15]. Modeling tools such as ADVISOR and PSAT are available in the public domain, which are discussed in more detail as follows.

III. HEV MODELING USING ADVISOR

ADvanced VehIcle SimulatOR (ADVISOR) is a modeling and simulation tool developed by U.S. National Renewable Energy Laboratory (NREL) [5], [6]. It can be used for the analysis of performance, fuel economy, and emissions of conventional, electric, hybrid electric, and fuel cell vehicles. The backbone of the ADVISOR model is the Simulink block diagram shown in Fig. 1, for a parallel HEV as an example. Each subsystem (block) of the block diagram has a Matlab file (m-file) associated with it, which defines the parameters of that particular subsystem. The user can alter both the model inside the block as well as the m-files associated with the block to suit the modeling needs. For example, the user may need a more precise model for the electric motor subsystem. A different model can replace the existing model as long as the inputs and the outputs are the same. On the other hand, the user may leave the model intact and only change the m-file associated with the block diagram. This is equivalent to choosing a different make of the same component (for example choosing a 12-Ah battery manufactured by Hawker-Genesis instead of a 6-Ah battery manufactured by Caterpillar). ADVISOR provides modeling flexibility for a user.

ADVISOR models fit empirical data obtained from the component testing to simulate a particular subsystem. In general, the efficiency and limiting performances define the operation of each component. For example, the ICE is modeled using an efficiency map that is obtained via experiments. The efficiency map of a Geo 1.0 L (43 kW) engine is shown in Fig. 2. The maximum torque curve is also shown in this map. The engine cannot perform beyond this maximum torque constraint. Maximum torque change is another constraint to the engine subsystem. In other

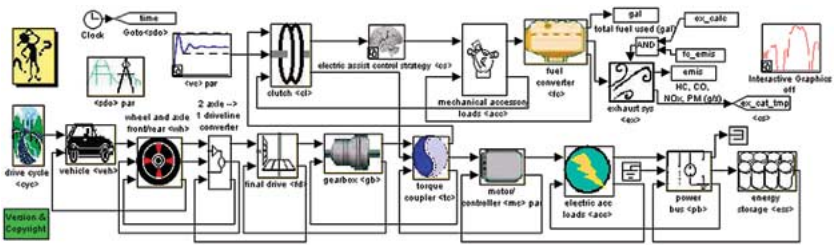

Fig. 1. *Block diagram of parallel HEV in ADVISOR.*

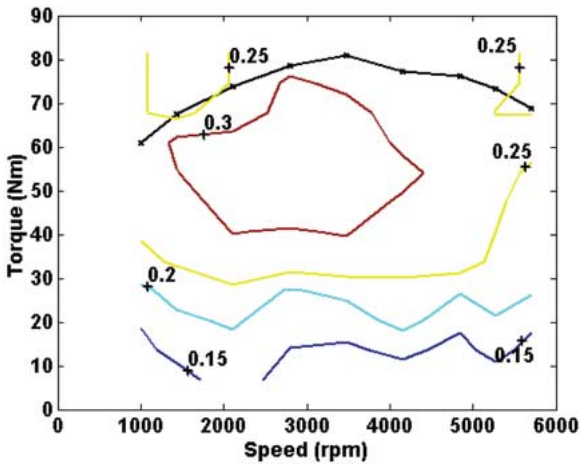

Fig. 2. *Geo 1.0 L (43 kW) SI engine efficiency map model.*

words, the model considers the inertia of the component in the simulation.

The program also allows for the linear scaling of components. For an ICE, this means linear scaling of the torque to provide the required maximum power. This type of scaling is valid only in the neighborhood near the actual parameter where the efficiency map for a slightly larger or smaller component would not change drastically. Scaling of the Geo ICE is shown in Fig. 3 so that the ICE gives a maximum power of 50 kW instead of the nominal 43 kW.

In the latest version of ADVISOR, the functionality of the software was improved by allowing links to other software packages such as Ansoft Simplorer [17] and Synopsys Saber [18]. These powerful software packages allow for a more detailed look at the electric systems of the vehicle.

As an application example, ADVISOR is used to simulate a hybrid battery/ultracapacitor energy storage system. More extensive applications can be found in [19], where ADVISOR is used to model hybrid fuel cell/battery powertrain and hybrid fuel cell/ultracapacitor powertrain and simulate their fuel economy and performance. The concept of using a hybrid energy storage system consisting of a battery and an ultra-capacitor (UC) is well known and well documented in literature [20], [21]. The ultra-capacitor provides and absorbs the current peaks, while the battery provides the average power required for the electric motor. This arrangement of hybrid energy storage in an HEV extends the life of the battery and allows the motor to operate more aggressively. Simulating such a system in ADVISOR allows the user to visualize the fuel economy benefit. At the same time, the program allows the user to design the best control strategy for the battery/ultra-capacitor hybrid to improve the battery life and the overall system performance. Finally, the size of the components can be optimized and, thus, the cost and weight of the system can be reduced.

The default battery model in ADVISOR operates by requesting a specific amount of power from the battery as decided by the vehicle control strategy. Depending on the amount of power that the battery is able to supply, the battery module will send out the power available from the battery to the other subsystems. Due to the hybrid backward/forward simulation method of ADVISOR, the amount of power that the batteries are able and required to supply in a given time step is calculated in a single iteration. From this value, the battery model calculates the battery variables like current, voltage, and the battery temperature.

However, a hybrid battery/ultracapacitor energy storage system cannot be modeled within ADVISOR using the above default battery model. Here, we have to replace the energy storage model with a more complex model. Fortunately, the subsystem model in ADVISOR can be altered as long as the types of inputs and outputs to the rest of the vehicle are not altered. In our simulation, we replaced the battery model by a model of a combination of a battery and an ultra-capacitor connected to a local control strategy unit that splits the power demand between the battery and the ultra-capacitor. Detailed information about the control strategy is available in [20]. The block diagram representation of the system is shown in Fig. 4.

The use of the model described gives the user a way to quickly and easily simulate the battery/ultra-capacitor subsystem in a vehicle environment. It allows the user to observe the benefit of using the ultra-capacitor on the fuel economy of the vehicle as well as the benefit to the battery by making the battery state of charge more even and by reducing the peaks of the battery current that the battery has to accept. It also allows the user to validate

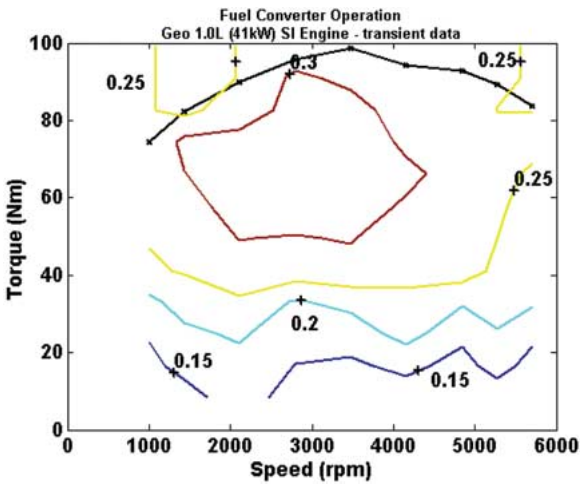

Fig. 3. *Geo 1.0 L engine scaled to give a maximum power of 50 kW by linear alteration of torque characteristics.*

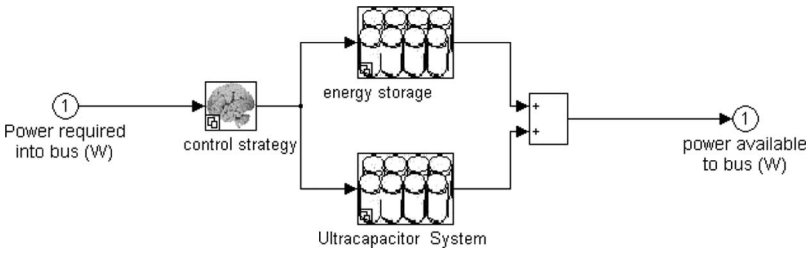

Fig. 4. ***Block diagram representation of new battery subsystem that consists of battery and ultra-capacitor. Input/output relation with rest of the system is left unchanged.***

the system whether it operates as efficiently if the battery size were reduced. Finally, the user can optimize the battery/ultra-capacitor control strategy (in other words, how the power demand will be split) without having to think about the complexities of designing the power electronics to make this control system feasible. In addition, the system can be optimized before any system is built and the system cost and possible savings can be easily calculated at the early design stage. Once the control strategy is optimized, the actual dc/dc converter with the required control strategies can be integrated into the simulation using Saber or Ansoft Simplorer software [20].

IV. HEV MODELING USING PSAT

The Powertrain System Analysis Toolkit (PSAT) is a state-of-the-art flexible simulation software developed by Argonne National Laboratory and sponsored by the U.S. Department of Energy (DOE) [7]. PSAT is modeled in a MATLAB/Simulink environment and is set up with a graphical user interface (GUI) written in C#, which makes it user friendly and easy to use. Being a forward-looking model, PSAT allows users to simulate more than 200 predefined configurations, including conventional, pure electric, fuel cell, and hybrids (parallel, series, power split, series-parallel). The large library of component data enables users to simulate light, medium, and heavy-duty vehicles.

The level of details in component models can be flexible, e.g., a lookup table model or high-fidelity dynamic model can be used for a component, depending on the user's simulation requirements. To maintain modularity, every model must have the same number of input and output parameters. The use of quasi-steady models and control strategies including the propelling, braking, and

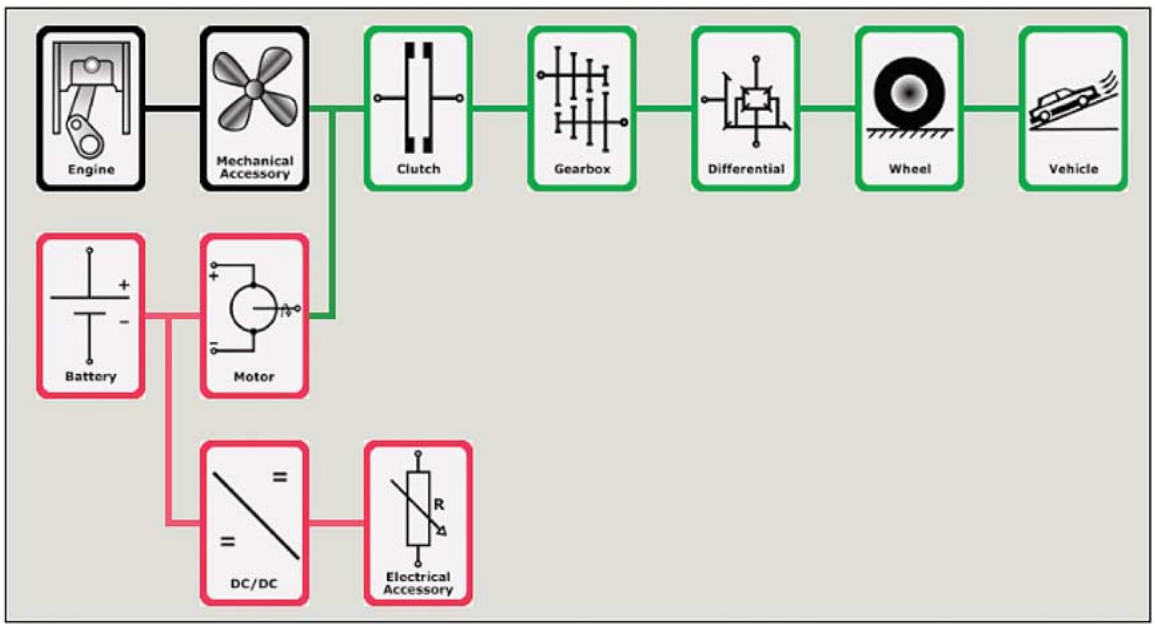

Fig. 5. ***Configuration of selected HEV in PSAT.***

Table 1 Parallel HEV Configuration

Component	Description
Fuel Converter	84 kW and 2.2 L Cavalier Gasoline Engine
Motor	ECOSTAR motor model with continuous power of 33 kW and peak power of 66 kW
Battery	NiMH Panasonic Battery with capacity 6.5 Ah and 240 cells
Transmission	4 speed manual gearbox with final drive ratio 3.63
Control Strategy	Propelling, Shifting and Braking (default)

shifting strategies in PSAT sets it apart from other steady-state simulation tools like ADVISOR. This feature makes PSAT predict fuel economy and performance of a vehicle more accurately. Its modeling accuracy has been validated against the Ford P2000 and Toyota Prius. PSAT is designed to cosimulate with other environments and is capable of running optimization routines. Hardware-in-the-loop (HIL) testing is made possible in PSAT with the help of PSAT-PRO, a control code to support the component and vehicle control [7].

As an application example, PSAT is used to optimize a parallel HEV for maximum fuel economy on a composite driving cycle. Four global algorithms, Divided RECTangle (DIRECT), Simulated Annealing (SA), Genetic Algorithm (GA), and Particle swarm optimization (PSO) are used in the model-based design optimization [23]. The vehicle model "gui_par_midsize_cavalier_ISG_in" (available in the PSAT model library) has been chosen for this optimization study. This vehicle is a two-wheel-drive starter-alternator parallel configuration with manual transmission. The basic configuration of the parallel HEV used for simulation is illustrated in Fig. 5 and main components are listed in Table 1.

The driving cycle is composed of city driving represented by FTP-75 (Federal Test Procedure) and the highway driving represented by HWFET (Highway Fuel Economy Test). The two drive cycles are shown in Fig. 6(a) and (b), respectively.

The fuel economy from each of these drive cycles is combined to get the composite fuel economy. By definition, composite fuel economy is the harmonic average of the SOC-balanced fuel economy values during the two separate drive cycles [22]. The composite fuel economy is calculated as given by the following formula:

$$\text{CompositeFuelEconomy} = \frac{1}{\frac{0.55}{\text{City}\_FE} + \frac{0.45}{\text{Hwy}\_FE}}$$

where City_*FE* and Hwy_*FE* represent the city and highway fuel economy values, respectively. Table 2 shows the six design variables used in this study. The first two define the power ratings of the fuel converter and motor controller. The third, fourth, and fifth variables define the number of battery modules, minimum battery state of charge (SOC) allowed, and maximum battery SOC allowed. The sixth design variable defines final drive ratio.

The following constraints are imposed on the design problem:

1) acceleration time 0−60 mph $<=$ 18.1 s;
2) acceleration time 40−60 mph $<=$ 7 s;
3) acceleration time 0−85 mph $<=$ 35.1 s;
4) maximum acceleration $>=$ 3.583 m/s^2.

First, the default vehicle with configuration given in Table 1 and the design variables given in Table 3 are

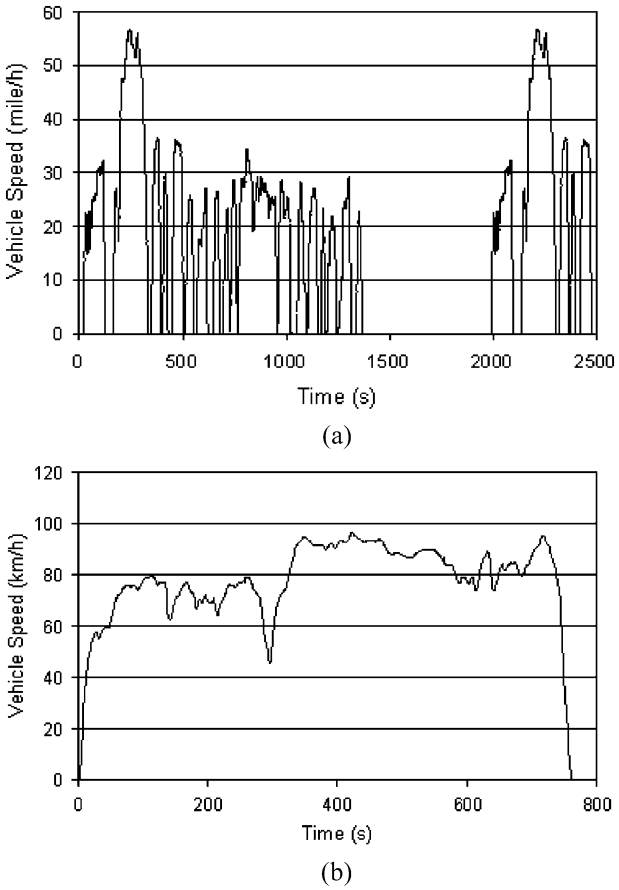

Fig. 6. *Drive cycles: (a) FTP-75 drive cycle and (b) HWFET drive cycle.*

Table 2 Upper and Lower Bounds of Design Variables

Design Variable	Description	Lower Bound	Upper Bound
eng.scale.pwr_max_des	Fuel converter power rating	40 kW	100 kW
mc.scale.pwr_max_des	Motor Controller power rating	10 kW	80 kW
ess.init.num_module	Battery number of cells	150	350
ess.init.soc_min	Minimum SOC allowed	0.2	0.4
ess.init.soc_max	Maximum SOC allowed	0.6	0.9
fd.init.ratio	Final drive ratio	2	4

simulated in PSAT. The fuel economy was observed to be 35.1 mpg given in Table 4 under the first column.

Second, the optimization algorithms, DIRECT, Simulated Annealing, Genetic Algorithms, and PSO, are looped with the PSAT Vehicle Simulator and the optimization is carried on. For this step, the same default vehicle configuration given in Table 1 is taken and the bounds for the design variables are taken as given in Table 2. The four algorithms are allowed to run for 400 function evaluations. Using the same number of function evaluations will allow us to compare the performance of the different algorithms. A comparison of the fuel economy before and after the optimization is given in Table 4. A significant improvement in the fuel economy is seen due to optimization (to a less extent in the case of PSO and GA, though). Of all the four algorithms, SA performs well with an improvement of 5 mpg approximately.

A comparison of the initial design variables and the optimum design variables found by the four optimization algorithms is given in Table 5. It is noticed that the power rating of the electric motor is reduced significantly after optimization.

All four optimization algorithms result in improved vehicle performance. The performance comparison of the HEV before and after the optimization is given in Table 6. It shows that the optimized vehicle performance is greatly improved compared to the unoptmized vehicle performance. The performance improvement by SA is far better compared to the other three algorithms.

The mass of the vehicle changes as the design variables change because the mass of the vehicle depends directly on the design variables. In particular, of the chosen six design variables, three design variables (power ratings of engine and motor, and energy modules) affect the mass of the vehicle. The mass of the vehicle before and after the optimization is given in Table 7. The mass of the vehicle decreased for DIRECT and SA while the vehicle weight increased slightly in the case of GA and PSO.

Table 3 Initial Design Variable Values

Design variable	Initial Value
eng.pwr_max_des	86 kW
mc.pwr_max_des	65.9 kW
ess.init.num_module	240
ess.init.soc_min	0
ess.init.soc_max	1
fd.init.ratio	3.63

V. PHYSICS-BASED MODELING

PSAT and ADVISOR are based on experiential models in the form of look-up tables and efficiency maps. The accuracy of these tools may not be good enough for vehicles operating under extreme conditions. For detailed dynamic modeling and simulation of HEV system, physics-based modeling is needed. VTB, PSIM, Simplorer, V-Elph are good examples of physics-based modeling tools, where the state variables of a component or subsystem are modeled according to the physical laws representing the underlying principles. The resulting model is a function of device parameters, physical constants, and variables. Such physics-based models can facilitate high fidelity simulations for dynamics at different time scales and also controller development.

In this section, the physics-based modeling technique, Resistive Companion Form (RCF) [24] modeling, in particular, is explored. The RCF method originates from electrical engineering but is suitable for multidisciplinary modeling applications such as hybrid powertrain.

A. RCF Modeling Technique

The RCF method has been used successfully in a number of industry-standard electronic design tools such as SPICE [25] and Saber. Recently, it has also been applied in the Virtual Test Bed [9], [24], which is being recognized as the leading software for prototyping of large-scale multitechnical dynamic systems. Using the Resistive Companion Form modeling technique, we can obtain high-fidelity physics-based models of each component in modular format. These models can be seamlessly

Table 4 Comparison of Fuel Economy

Fuel Economy				
Before Optimization	After Optimization			
	DIRECT	SA	GA	PSO
35.1 mpg	39.64 mpg	40.37 mpg	37.6 mpg	37.1 mpg

Table 5 Final Design Variable Values

Design variable	Initial Value	Final Value			
		DIRECT	SA	GA	PSO
eng.pwr_max_des	86 kW	83.1 kW	82.4 kW	95.5 kW	87.1 kW
mc.pwr_max_des	65.9 kW	20.2 kW	21.9 kW	24.2 kW	14.8 kW
ess.init.num_module	240	245	311	300	238
ess.init.soc_min	0	0.25	0.22	0.34	0.26
ess.init.soc_max	1	0.84	0.78	0.89	0.78
fd.init.ratio	3.63	3.9	4.0	3.49	3.42

Table 6 Comparison of HEV Performance

Constraint	Constr. Value	Before Opt.	After Opt.			
			DIRECT	SA	GA	PSO
0 – 60 mph	<=18.1 s	18.1 s	15.5 s	10.8 s	11.9 s	11.1 s
40 – 60 mph	<=7 s	7 s	6.8 s	5 s	4.4 s	4.9 s
0 – 85 mph	<=35.1 s	35.1 s	30.6 s	20.7 s	21.2 s	20 s
Max. Accel.	>=3.583 m/s^2	3.583 m/s^2	3.97 m/s^2	4.07 m/s^2	3.94 m/s^2	3.99 m/s^2

Table 7 Mass of HEV Before and After Optimization

Mass of the vehicle				
Before Optimization	After Optimization			
	DIRECT	SA	GA	PSO
1683 kg	1635 kg	1656 kg	1694 kg	1690 kg

integrated to build a system simulation model suitable for design. Just as a physical device is connected to other devices to form a system, the device can be modeled as a block with a number of terminals through which it can be interconnected to other component models, as shown in Fig. 7. Each terminal has an associated across and a through variable. If the terminal is electrical, these variables are the terminal voltage with respect to a common reference and the electrical current flowing into the terminal, respectively. Notice that the concept of across and through variables in RCF is similar to the effort/flow concepts used in ADVISOR and PSAT.

The general form of the RCF model can be expressed as follows, which is obtained by numerically integrating the

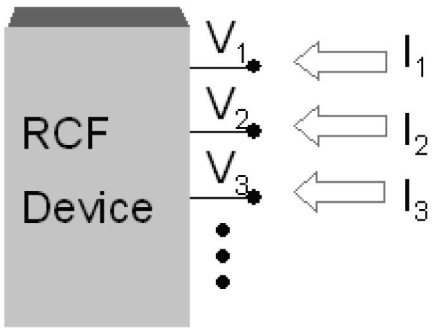

Fig. 7. ***Physics-based RCF modeling technique.***

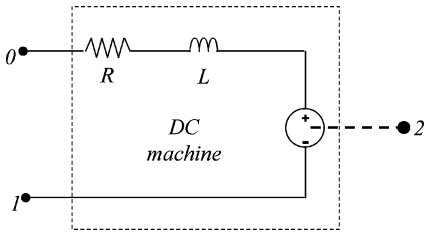

Fig. 8. ***DC machine modeling.***

differential-algebraic equations describing the dynamics of the component:

$$\begin{bmatrix}\mathbf{i}(t)\\ \mathbf{0}\end{bmatrix} = \mathbf{G}[\mathbf{v}(t),\ \mathbf{v}(t-h),\ \mathbf{i}(t),\ \mathbf{i}(t-h),\ \mathbf{y}(t),\ \mathbf{y}(t-h), t] \times \begin{bmatrix}\mathbf{v}(t)\\ \mathbf{y}(t)\end{bmatrix} - \begin{bmatrix}\mathbf{b}_1[\mathbf{v}(t),\mathbf{v}(t-h),\mathbf{i}(t),\mathbf{i}(t-h),\mathbf{y}(t),\mathbf{y}(t-h),t]\\ \mathbf{b}_2[\mathbf{v}(t),\mathbf{v}(t-h),\mathbf{i}(t),\mathbf{i}(t-h),\mathbf{y}(t),\mathbf{y}(t-h),t]\end{bmatrix} \tag{1}$$

where i is a vector of through variables; v is a vector of across variables; y is a vector of internal state variables; h is the numerical integration time step; G is a Jacobian matrix; and b_1 and b_2 are vectors depending in general on past history values of through, across variables and internal states and on values of these quantities at time instant t. Note that G, b_1, and b_2 depend on the chosen integration method. The most common integration methods that can be used are the trapezoidal rule and second-order Gear's method.

After all the powertrain components are modeled in RCF, they can be integrated into one set of algebraic equations by applying the connectivity constraints between neighboring modular components, which can then be solved to get system state variables.

B. Hybrid Powertrain Modeling

Modeling examples for powertrain components are given for a dc machine, a dc/dc boost power electronic converter, and vehicle dynamics. Through these modeling examples, the principles of physics-based modeling techniques are demonstrated. Extensive covering of models for all the powertrain components are not intended.

1) Modeling of DC Machine: An equivalent circuit model of the dc machine is illustrated in Fig. 8, where R and L are the armature resistance and inductance, respectively. The dc machine has two electrical terminals (0,1) and one mechanical terminal (2).

The through variables are: $i = [i_0, i_1, T_{sh}]^t$, where $T_{sh}(= i_2)$ is the mechanical torque at the machine shaft; and the superscript "t" indicates matrix transpose. The across variables are: $v = [v_0, v_1, \omega]^t$, where $\omega(= v_2)$ is the rotational speed of the machine shaft.

The differential algebraic equations describing the machine dynamics are

$$\begin{cases} i_0 = -\frac{L}{R}\frac{di_0}{dt} + \frac{1}{R}(v_0 - v_1) - \frac{k_e\phi}{R}v_2 \\ i_1 = -i_0 \\ i_2 = -(k_T\phi)i_0 + J\frac{dv_2}{dt} + d \bullet v_2 \end{cases} \tag{2}$$

where J is shaft inertia, d is the drag coefficient, and Φ is the flux per pole. Applying the trapezoidal integration rule, we can get the following RCF model:

$$i(t) = G(h) \bullet v(t) - b(t-h) \tag{3}$$

where

$$G(h) = \begin{bmatrix} \frac{h}{hR+2L} & \frac{-h}{hR+2L} & \frac{-hk_e\phi}{hR+2L} \\ \frac{-h}{hR+2L} & \frac{h}{hR+2L} & \frac{hk_e\phi}{hR+2L} \\ \frac{-hk_T\phi}{hR+2L} & \frac{hk_T\phi}{hR+2L} & \left(\frac{hk_e\phi k_T\phi}{hR+2L} + \frac{2J}{h}\right) \end{bmatrix} \tag{4}$$

$$b(t-h) = \begin{bmatrix} b_0(t-h) \\ -b_0(t-h) \\ b_2(t-h) \end{bmatrix} \tag{5}$$

$$b_0(t-h) = \frac{hR-2L}{hR+2L}i_0(t-h) - \frac{h}{hR+2L}v_0(t-h) + \frac{h}{hR+2L}v_1(t-h) + \frac{hk_e\phi}{hR+2L}v_2(t-h) \tag{6}$$

$$b_2(t-h) = -k_T\phi b_0(t-h) + k_T\phi i_0(t-h) + i_2(t-h) + \frac{2J}{h}v_2(t-h). \tag{7}$$

2) Modeling of DC/DC Boost Converter: An equivalent circuit model of the dc/dc Boost Converter is illustrated in Fig. 9. The dc/dc Boost Converter has three electrical terminals (0, 1, 2). Here, we derive the average state space

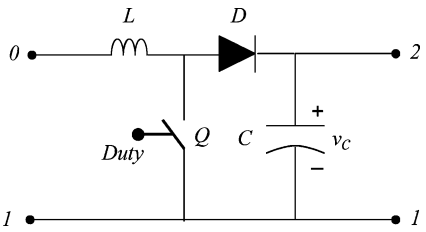

Fig. 9. ***DC/DC boost converter modeling.***

model, based on the two states of the circuit when the switch is ON or OFF.

When the switch Q is ON, we have the following state-space dynamic equations:

$$\begin{aligned}\frac{di_0}{dt} &= \frac{1}{L}(v_0 - v_1)\\ \frac{d(v_2 - v_1)}{dt} &= \frac{1}{C} i_2.\end{aligned} \tag{8}$$

When the switch Q is OFF, we have the following state-space dynamic equations:

$$\begin{aligned}\frac{di_0}{dt} &= \frac{1}{L}(v_0 - v_2)\\ \frac{d(v_2 - v_1)}{dt} &= \frac{1}{C}(i_0 + i_2).\end{aligned} \tag{9}$$

Hence, the Middlebrook state-space averaging model is (d = duty) as follows:

$$\begin{aligned}\frac{di_0}{dt} &= \frac{d}{L}(v_0 - v_1) + \frac{(1-d)}{L}(v_0 - v_2)\\ \frac{d(v_2 - v_1)}{dt} &= \frac{d}{C} i_2 + \frac{(1-d)}{C}(i_0 + i_2).\end{aligned} \tag{10}$$

Applying the trapezoidal integration rule, we can get the following RCF model for the boost power converter:

$$i(t) = G(h) \bullet v(t) - b(t-h) \tag{11}$$

where

$$G(h) = \begin{bmatrix} \frac{h}{2L} & \frac{-hd}{2L} & \frac{-h(1-d)}{2L} \\ \frac{-hd}{2L} & \frac{hd^2}{2L} + \frac{2C}{h} & \frac{hd(1-d)}{2L} - \frac{2C}{h} \\ \frac{-h(1-d)}{2L} & \frac{hd(1-d)}{2L} - \frac{2C}{h} & \frac{hd(1-d)^2}{2L} + \frac{2C}{h} \end{bmatrix} \tag{12}$$

$$b(t-h) = \begin{bmatrix} b_0(t-h) \\ -b_0(t-h) - b_2(t-h) \\ b_2(t-h) \end{bmatrix} \tag{13}$$

$$\begin{aligned} b_0(t-h) = &-i_0(t-h) - \frac{h}{2L} v_0(t-h) \\ &+ \frac{hd}{2L} v_1(t-h) + \frac{h(1-d)}{2L} v_2(t-h) \end{aligned} \tag{14}$$

$$\begin{aligned} b_2(t-h) = &-(1-d) b_0(t-h) + (1-d) i_0(t-h) \\ &+ i_2(t-h) - \frac{2C}{h} v_1(t-h) + \frac{2C}{h} v_2(t-h). \end{aligned} \tag{15}$$

3) Modeling of Vehicle Dynamics: The vehicle dynamic model can be derived from Newton's Second law considering all the forces applied upon the vehicle. The driving force comes from the powertrain shaft torque, which can be written as the wheel torque

$$T_{\text{wh}} = R_g \eta_{\text{trans}} T_{\text{sh}} \tag{16}$$

where R_g and η_{trans} are the transmission gear ratio and transmission efficiency, respectively. This wheel torque provides the driving force to the vehicle

$$F_d = \frac{T_{\text{wh}}}{r} \tag{17}$$

where r is the wheel radius.

The total resistance force consists of rolling resistance, aerodynamic resistance, and gravitational force. Hence, the vehicle dynamic equation can be obtained as

$$\begin{aligned} F_d &= F_{\text{gxt}} + F_{\text{roll}} + F_{\text{ad}} + ma \\ &= mg\sin(\alpha) + mg(C_0 + C_1 v) * \text{sgn}(v) \\ &\quad + \frac{1}{2}\rho C_d A_F (v + v_0)^2 * \text{sgn}(v) + \left(m + \frac{J_{\text{wh}}}{r^2}\right)\frac{dv}{dt} \end{aligned} \tag{18}$$

where F_{gxt} is the gravitational force on a grade, F_{roll} is rolling resistance, F_{ad} is the aerodynamic resistance, m is the vehicle mass, g is the natural acceleration, α is the angle of grade, C_0 and C_1 are the rolling coefficients, ρ is the air density, C_d is the aerodynamic drag coefficient, A_F is the vehicle frontal area, v_0 is the wind speed, v is the vehicle linear speed, and J_{wh} is the wheel inertia.

Similarly, applying the trapezoidal integration rule, we can get the following RCF model for the vehicle dynamics:

$$i(t) = G(h) \bullet v(t) - b(t-h) \tag{19}$$

where the through variable is $i(t) = F_d$ and the across variable $v(t) = v$ (vehicle velocity).

Note that (18) is a nonlinear model, requiring an iterative Newton–Raphson solution procedure at each simulation time step; the Jacobian $G(h)$ is as follows:

$$\begin{aligned} G(h, v(t)) = &\, mgC_1 \text{sgn}(v) + \rho C_d A_F (v(t) + v_0)\text{sgn}(v) \\ &+ \frac{2}{h}\left(m + \frac{J_{\text{wh}}}{r^2}\right). \end{aligned} \tag{20}$$

Other RCF models for induction machine, batteries, ultracapacitors, etc., can be found in [24], [26], and [27]

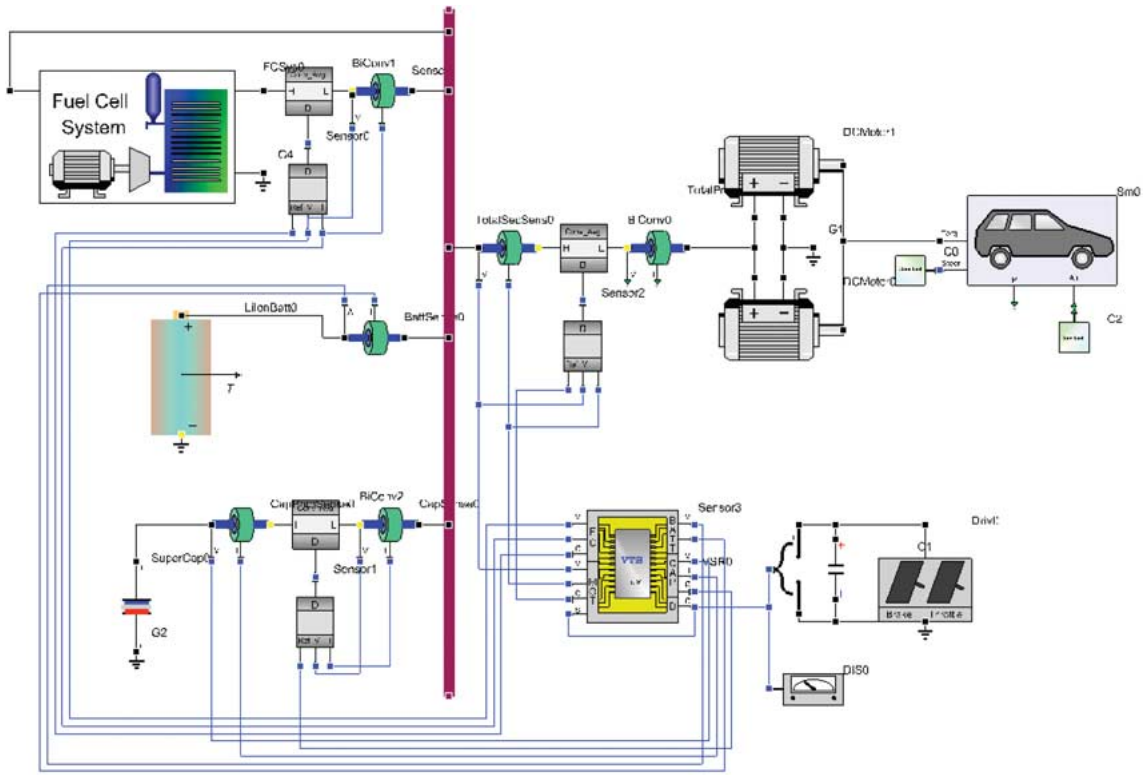

Fig. 10. *Modeling a hybrid fuel cell/ultracapacitor/battery vehicle in VTB [9].*

respectively. Based on the same principles, the internal combustion engine model and fuel cell model can be developed.

Finally, as an example of employing RCF techniques for HEVs, a hybrid fuel cell/ultracapacitor/battery vehicle model is modeled in VTB [9], as shown in Fig. 10. Upon simulation, variables that are of interest can be plotted, as shown in Fig. 11, where the reference vehicle speed, battery, ultracapacitor, and dc motor currents are plotted. Details of how to use VTB can be found in [9].

C. Wheel Slip Model

In simulations where it involves vehicle dynamics, the wheel slip model must be implemented. Fig. 12 shows the one-wheel model of the HEV. Applying a driving torque or a braking force F_m to a pneumatic tire produces tractive (braking) force F_d at the tire-ground contact patch due to the wheel slip. The slip ratio λ is defined as

$$\lambda = \frac{V_\omega - V}{\max\{V, V_\omega\}} \tag{21}$$

where V is the vehicle speed and V_ω is the linear speed of the wheel.

The wheel speed can be expressed as

$$V_\omega = \omega r \tag{22}$$

where ω is the angular speed of the wheel and r is the radius of the wheel.

During normal driving, $\lambda > 0$, there exists a friction force on the wheel in the direction of the forward motion. This friction force, also known as traction force, is caused by the slip between the road surface and the tire. This force contributes to the forward motion of the vehicle during normal driving. During braking, external forces are applied to the wheel so that the wheel linear speed is less than the vehicle speed, e.g., $\lambda < 0$. Therefore, there exists a braking force opposite to the forward motion.

The traction force, or braking force in the case of braking, can be expressed as follows:

$$F_d(\lambda) = \mu(\lambda) mg \tag{23}$$

where $\mu(\lambda)$ is the adhesive coefficient between the road surface and the tire. $\mu(\lambda)$ is a function of slip ratio λ and is a function of tire condition and road condition as shown in Fig. 13.

The equation of the vehicle motion can be expressed as

$$m\frac{dV}{dt} = F_d(\lambda) - (F_{\text{gxt}} + F_{\text{ad}} + F_{\text{roll}}). \tag{24}$$

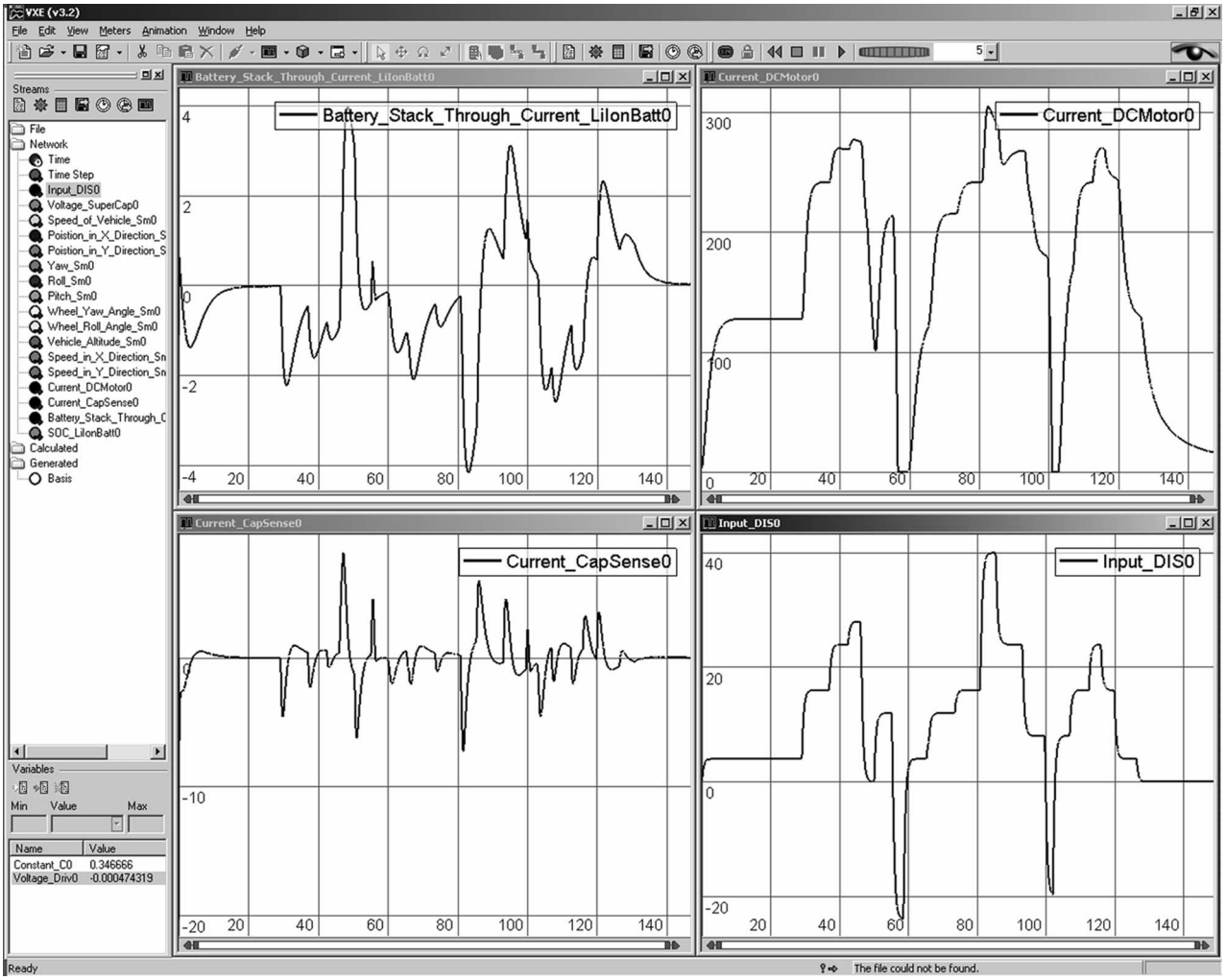

Fig. 11. ***Simulation results of hybrid vehicle in VTB.***

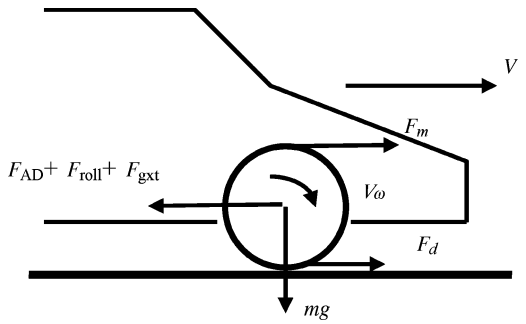

Fig. 12. ***One wheel model of vehicles, where F_m is the force applied to the wheel by the powertrain, F_d is the tractive force caused by tire slip, m is the vehicle mass, and g is the natural acceleration rate.***

This equation is similar to (18) but the tractive force is linked with slip ratio.

During normal driving, the external torque applied to the wheels is positive. In order to enter braking mode, an external torque must be applied to the wheel to slow down the wheel. In HEV, this torque is the sum of the motor regenerative braking torque and additional braking torque provided by the mechanical braking systems, in case the motor torque is not enough to provide effective braking.

During normal driving, the powertrain torque tries to accelerate the wheel while the tractive force will try to slow down the wheel. During braking, the powertrain torque applied to the wheel is in the opposite direction of the wheel rotation and slows down the wheel. The traction force, on the other hand, is in the same direction as the

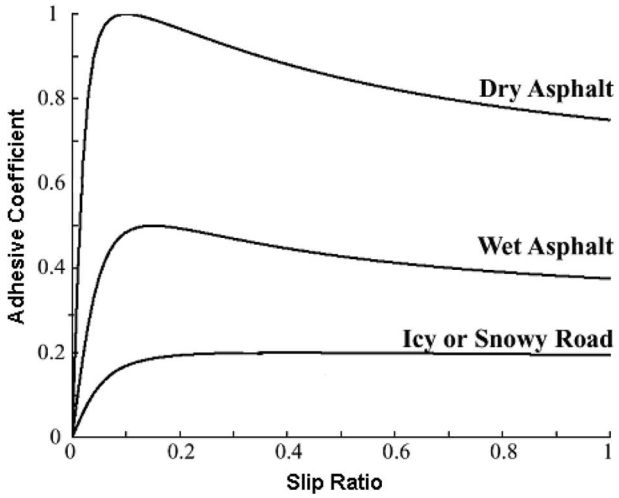

Fig. 13. *Typical adhesive coefficient between road surface and tires, as a function of slip ratio and road surface conditions.*

wheel rotation and therefore will accelerate the wheel, as shown in Fig. 12.

Therefore, the equation of the wheel motion can be expressed as follows:

$$J_\omega \frac{d\omega}{dt} = T_m - rF_d(\lambda) \tag{25}$$

where J_ω is the wheel inertia, T_m is the total braking torque, and $T_m = F_m * r$.

VI. BOND GRAPH AND OTHER MODELING TECHNIQUES

A. Bond Graph Modeling for HEV

Created by H. M. Paynter in 1959, bond graphs are a graphical tool used to describe and model subsystem interactions involving power exchange. This formulation can be used in hydraulics, mechatronics, and thermodynamic and electrical systems. The bond graph has been proven effective for the modeling and simulation of multidomain systems including automotive systems [28]–[39].

In a Bond Graph model, a physical system is represented by basic passive elements that are able to interchange power: *resistances (R)*, *capacitances (C)*, and *inertias (I)*. Although these names suggest a direct application in electrical systems, they are used in any other domains as well, e.g., friction as a mechanical resistance, a compressible fluid as a capacitance, and a flywheel as an inertial element.

Each element has one or more ports where power exchange can occur. This *power (P)* is expressed as a product of two variables: *effort (e)* and *flow (f)*. These names are used extensively in all domains but have a unique name on each domain: force and speed in mechanical, voltage and current in electrical, pressure and flow in hydraulics, and so on. Additional variables are defined: *momentum (p)* as the time integral of effort and *displacement (q)* as the time integral of flow.

Additional elements are needed to fully describe a system: *sources of effort* (S_e) and *sources of flow* (S_f) are active elements that provide the system with effort and flow respectively; *transformers (TF)* and *gyrators (GY)* are two-port elements that transmit power, but scale their effort and flow variables by its modulus; and *one junction* (1) elements are multiport elements that distribute power sharing equal flow, while *zero junction* (0) elements distribute power, having equal effort among all ports.

Bond graph elements are linked with half arrows (bonds) that represent power exchange between them. The direction of the arrow indicates the direction of power flow when both effort and flow are positive. Full arrows are used when a parameter is to be passed between elements, but no power flow occurs.

A bond graph can be generated from the physical structure of the system. For example, the HEV powertrain connected to a road load model can be drawn as shown in Fig. 14, where the road load is described by (18).

Causality in Bond Graph models is indicated with a vertical stroke at the start or end of the bond arrow. This causal stroke establishes the cause and effect relationships between elements. Causality in bond graphs enables the extraction of system dynamics equations. It also provides an insight of the dynamic behavior or the model and is useful to predict modeling problems such as algebraic loops, differential causality, and causal loops.

Modeling presented in [38] and [39] demonstrated that Bond Graph modeling is an appropriate method for the modeling and simulation of hybrid and electric vehicles.

B. HEV Modeling Using PSIM

PSIM is a user-friendly simulation package that was originally developed for simulating power electronic converters and electric machine drives. Its new version allows interactive simulation capability and provides magnetics and thermal models for more flexible and accurate analysis of automotive mechatronics design. However, with a few additional customer-built models, it can also be used to model and simulate electric and hybrid vehicles.

Module boxes for necessary electrical systems and also mechanical, energy storage, and thermal systems are created. These modules include internal combustion engines, fuel converters, transmissions, torque couplers, and batteries. Once these modules are made and stored in the PSIM model library, the user can build an electric or a hybrid vehicle model. As an example, a series hybrid configuration, shown in Fig. 15, is modeled in PSIM [40].

Since load torque is imposed only on the propulsion motor, the ICE can be operated at its optimal efficiency all

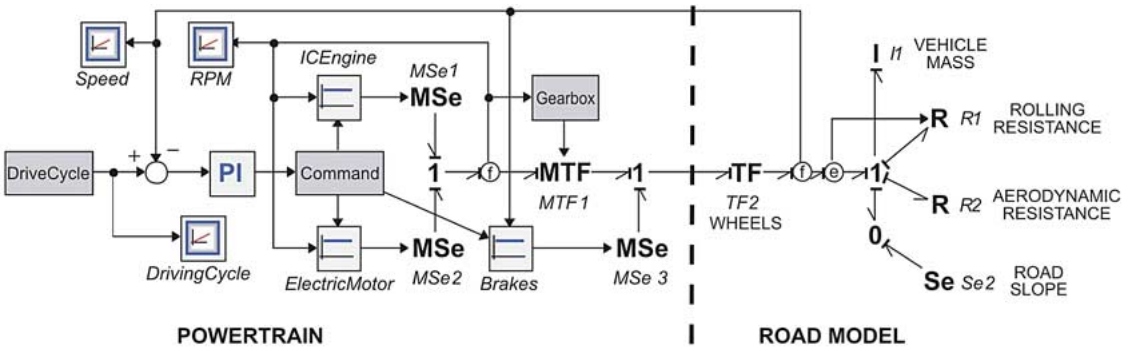

Fig. 14. *Bond graph modeling example: HEV powertrain model connected to road model.*

the time regardless of the load torque. Therefore, energy management strategy is simple. The main design task is focused on how and where to operate the ICE at an optimum region [40], [41].

Simulation results of the engine speed for the UDDS drive cycle are presented in Fig. 16.

This simulation model assumed that the power produced by the engine is equal to the power generated by the generator and stored directly into the battery. It can be observed that power is produced when the engine is on (Fig. 17).

C. HEV Modeling Using Simplorer and V-ELPH

Simplorer is a multidomain simulation package that can be used for system-level HEV modeling. It has a comprehensive automotive component library, including batteries, fuel cells, wires, fuses, lamps, electrical motors, alternators, engine models, relays, in addition to the electronics, power electronics, and controller models. Further, Simplorer can be linked for co-simulation with a finite-element-based electromagnetic field simulation package, Maxwell [17]. This capability provides even greater modeling and simulation accuracy for automotive electronics and machine design. In [42], a series hybrid electric HMMWV is modeled in Simplorer. The vehicle model consists of an ICE/generator, a PM dc motor, a dc/dc converter, a battery and battery management system, PI controller, and vehicle model. The simulation facilitates the development and functional verification of controller and battery management. Dynamic/transient responses of battery voltage, motor torque, and motor voltage under different drive cycles can be simulated. Also, the vehicle's response for incline of road grades can be obtained to predict overall system performance.

V-Elph [12] is a system level Matlab/Simulink-based modeling, simulation, and analysis tool developed at Texas A & M University. This package uses detailed dynamic models of electric motors, internal combustion engines,

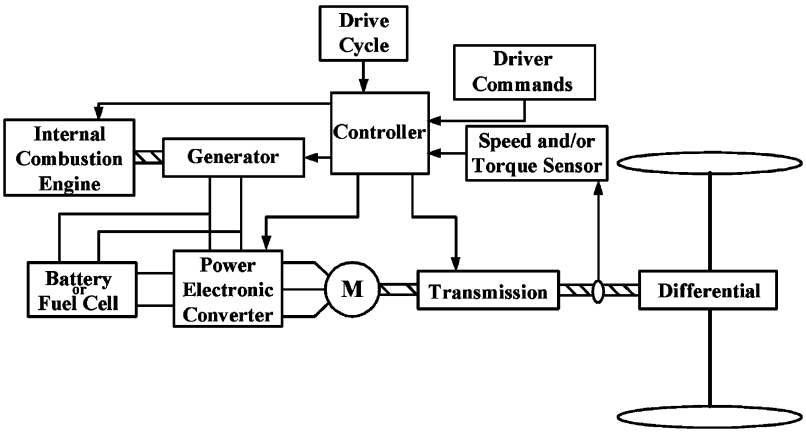

Fig. 15. *Series HEV configuration.*

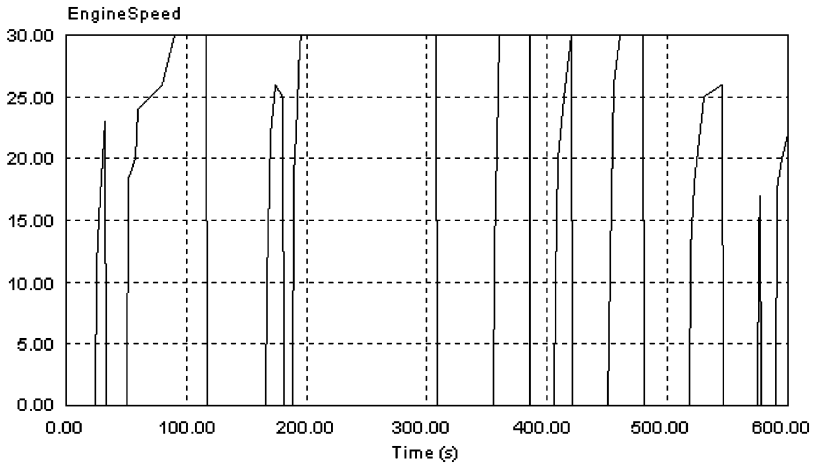

Fig. 16. ***Engine speed (× 100 rpm) versus time in seconds.***

batteries, and vehicle. The dynamic performance and fuel economy, energy efficiency, emissions, etc., can be predicted for hybrid and electric vehicles.

In addition, software packages, such as Modelica [43], [44] and Saber [45], are also used in the physics-based modeling and simulation of hybrid and electric vehicles.

VII. CONSIDERATION OF NUMERICAL INTEGRATION METHODS

Numerical integration of differential equations or state equations is essential for performing dynamic system simulation. Therefore, discussion of numerical integration methods is an integral part of a paper focusing on modeling and simulation. There are a variety of numerical integration methods: backward Euler's, trapezoidal, Simpson's, Runge-Kutta's, Gear's methods, etc. Among these methods, trapezoidal integration is the most popular one in dynamic modeling and simulation due to its merits of low distortion and absolute-stability (A-stable). For example, the trapezoidal integration rule is used in EMTP, Spice, and Virtual Test Bed. However, numerical oscillations are often encountered, especially in the simulation of power electronics circuits, which are used very often in hybrid powertrains. Specifically, the numerical values of certain variables oscillate around the true values. In other words, only the average values of the simulated results are correct. The magnitude and frequency of these numerical oscillations are directly related to the parameters of the energy storage elements and the simulation time step. Sometimes, this problem is so severe that the simulation results are erroneous.

Two techniques can be used to mitigate the problem of this kind of numerical oscillations: trapezoidal with

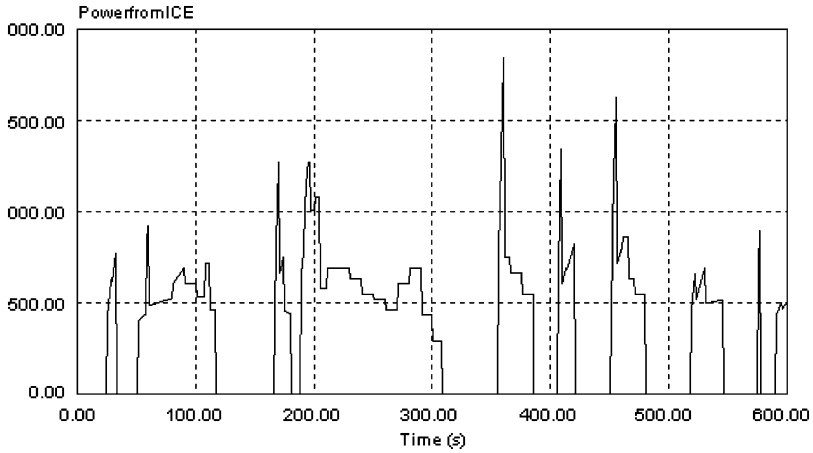

Fig. 17. ***Power (× 100 W) from the ICE versus time in seconds.***

numerical stabilizer method and Gear's second-order method. Elimination of numerical oscillations is of great significance in performing a meaningful simulation for power electronics circuits in which switching of semiconductor devices cause current interruptions.

VIII. CONCLUSION

This paper has presented an overview of the modeling and simulation of HEV, with specific emphasis on physics based modeling. Methods for the mitigation of numerical oscillations in dynamic digital simulations are briefly discussed. Additional simulation techniques, such as Bond Graph modeling, provide added flexibility in HEV modeling and simulation.

With the advent of powerful computing, development of computational methods, and advances in software-in-the-loop (SIL) and hardware-in-the-loop (HIL) modeling and simulations, it is now possible to study numerous iterations of different designs with the combinations of different components and different topology configurations. HIL is becoming increasingly important for rapid prototyping and development of control system for new vehicles such as X-by-Wire [46].

With the ever more stringent constraints on energy resources and environmental concerns, HEV will attract more interest from the automotive industry and the consumer. Although the market share is still insignificant today, it can be predicted that HEV will gradually gain popularity in the market due to the superior fuel economy and vehicle performance. Modeling and simulation will play important roles in the success of HEV design and development. ■

Acknowledgment

The authors would like to acknowledge M. O'Keefe and K. Kelly of the U.S. National Renewable Energy Laboratory who have provided some original material for the manuscript. The authors would also like to thank Dr. C. C. Chan for his support of this paper.

REFERENCES

[1] K. Muta, M. Yamazaki, and J. Tokieda, "Development of new-generation hybrid system THS II—Drastic improvement of power performance and fuel economy," presented at the SAE World Congr., Detroit, MI, March 8–11, 2004, SAE Paper 2004-01-0064.

[2] T. Horie, "Development aims of the new CIVIC hybrid and achieved performance," in *Proc. SAE Hybrid Vehicle Technologies Symp.*, San Diego, CA, Feb. 12, 2006.

[3] P. Struss and C. Price, "Model-based systems in the automotive industry," *AI Mag.*, vol. 24, no. 4, pp. 17–34, Winter 2004.

[4] W. Gao *et al.*, "Hybrid powertrain design using a domain-specific modeling environment," in *Proc. IEEE Vehicle Power Propulsion Conf.*, Chicago, IL, Sep. 2005, pp. 6–12.

[5] K. B. Wipke, M. R. Cuddy, and S. D. Burch, "ADVISOR 2.1: A user-friendly advanced powertrain simulation using a combined backward/forward approach," *IEEE Trans. Vehicular Technol.*, vol. 48, no. 6, pp. 1751–1761, Nov. 1999.

[6] T. Markel, A. Brooker, T. Hendricks, V. Johnson, K. Kelly, B. Kramer, M. O'Keefe, S. Sprik, and K. Wipke, "ADVISOR: A systems analysis tool for advanced vehicle modeling," *J. Power Sources*, vol. 110, no. 2, pp. 255–266, Aug. 2002.

[7] PSAT Documentation. [Online]. Available: http://www.transportation.anl.gov/software/PSAT/

[8] PSIM Website. [Online]. Available: http://www.powersimtech.com/

[9] VTB Website. [Online]. Available: http://vtb.ee.sc.edu/

[10] B. Powell, K. Bailey, and S. Cikanek, "Dynamic modeling and control of hybrid electric vehicle powertrain systems," *IEEE Contr. Sys. Mag.*, vol. 18, no. 5, pp. 17–22, Oct. 1998.

[11] C. C. Lin, Z. Filipi, Y. Wang, L. Louca, H. Peng, D. Assanis, and J. Stein, "Integrated, feed-forward hybrid electric vehicle simulation in Simulink and its use for power management studies," in *Proc. SAE 2001 World Congr.*, Detroit, MI, Mar. 2001.

[12] K. L. Butler, M. Ehsani, and P. Kamath "A Matlab-based modeling and simulation package for electric and hybrid electric vehicle design," *IEEE Trans. Vehicular Technol.*, vol. 48, no. 6, pp. 1770–1118, Nov. 1999.

[13] G. Rizzoni, L. Guzzella, and B. M. Baumann, "United modeling of hybrid electric vehicle drivetrains," *IEEE Trans. Mechatronics*, vol. 4, no. 3, pp. 246–257, 1999.

[14] X. He and J. W. Hodgeson, "Modeling and simulation for hybrid electric vehicles, I. Modeling," *IEEE Trans. Intelligent Transportation Syst.*, vol. 3, no. 4, pp. 235–243.

[15] X. He and J. Hodgson, "Modeling and simulation for hybrid electric vehicles—Part II," *IEEE Trans. Transportation Syst.*, vol. 3, no. 4, pp. 244–251, Dec. 2002.

[16] P. Fritzson, *Principles of Object Oriented Modeling and Simulation With Modelica 2.1.* Piscataway, NJ: IEEE Press, 2004.

[17] Ansoft Simplorer Website. [Online]. Available: http://www.ansoft.com/

[18] Saber Website. [Online]. Available: http://www.synopsys.com/saber/

[19] W. Gao, "Performance comparison of a hybrid fuel cell—Battery powertrain and a hybrid fuel cell—Ultracapacitor powertrain," *IEEE Trans. Vehicular Technol.*, vol. 54, no. 3, pp. 846–855, May 2005.

[20] A. C. Baisden and A. Emadi, "An ADVISOR based model of a battery and an ultra-capacitor energy source for hybrid electric vehicles," *IEEE Trans. Vehicular Technol.*, vol. 53, no. 1, Jan. 2004.

[21] B. K. Bose, M. H. Kim, and M. D. Kankam, "Power and energy storage devices for next generation hybrid electric vehicle," in *Proc. 31st Intersociety Energy Conversion Engineering Conf.*, 1996, vol. 3, pp. 1893–1898.

[22] K. Wipke, T. Markel, and D. Nelson, "Optimizing energy management strategy and a degree of hybridization for a hydrogen fuel cell SUV," in *Proc. 18th Electric Vehicle Symp. (EVS-18)*, Berlin, Germany, Oct. 20–24, 2001.

[23] W. Gao and S. Porandla, "Design optimization of a parallel hybrid electric powertrain," in *Proc. IEEE Vehicle Power Propulsion Conf.*, Chicago, IL, Sep. 2005, pp. 530–535.

[24] W. Gao, E. Solodovnik, and R. Dougal, "Symbolically-aided model development for an induction machine in Virtual Test Bed," *IEEE Trans. Energy Conversion*, vol. 19, no. 1, pp. 125–135, Mar. 2004.

[25] SPICE Website. [Online]. Available: http://bwrc.eecs.berkeley.edu/Classes/IcBook/SPICE/

[26] L. Gao, S. Liu, and R. A. Dougal, "Dynamic lithium-ion battery model for system simulation," *IEEE Trans. Components Packaging Technol.*, vol. 25, no. 3, pp. 495–505, Sep. 2002.

[27] L. Gao, S. Liu, and R. A. Dougal, "Active power sharing in hybrid battery/capacitor power sources," in *Appl. Power Electronics Conf. Expo.*, 2003, vol. 1, pp. 497–503.

[28] S. Xia, D. A. Linkens, and S. Bennett, "Automatic modeling and analysis of dynamic physical systems using qualitative reasoning and bond graphs," *Intelligent Syst. Eng.*, vol. 2, pp. 201–212, Autumn, 1993.

[29] G. L. Gissinger, Y. Chamaillard, and T. Stemmelen, "Modeling a motor vehicle and its braking system," *J. Math. Computers Simulation*, vol. 39, pp. 541–548, 1995.

[30] K. Suzuki and S. Awazu, "Four-track vehicles by bond graph-dynamic characteristics of four-track vehicles in snow," in *Proc. 26th Ann. Conf. IEEE Industrial Electronics Soc. IECON 2000*, Oct. 2000, vol. 3, pp. 1574–1579.

[31] J.-H. Kim and D. D. Cho, "An automatic transmission model for vehicle control," in *Proc. IEEE Conf. Intelligent Transportation System, ITSC 97*, Nov. 1997, pp. 759–764.

[32] N. Nishijiri, N. Kawabata, T. Ishikawa, and K. Tanaka, "Modeling of ventilation system for vehicle tunnels by means of bond graph," in *Proc. 26th Ann. Conf. IEEE Industrial Electronics Soc., IECON 2000*, Oct. 2000, vol. 3, pp. 1544–1549.

[33] M. L. Kuang, M. Fodor, D. Hrovat, and M. Tran, "Hydraulic brake system modeling and control for active control of vehicle

dynamics," in *Proc. 1999 Amer. Contr. Conf.*, Jun. 1999, vol. 6, pp. 4538–4542.

[34] M. Khemliche, I. Dif, S. Latreche, and B. O. Bouamama, "Modeling and analysis of an active suspension 1/4 of vehicle with bond graph," in *Proc. First Int. Symp. Control, Communications Signal*, Mar. 2004, pp. 811–814.

[35] A. J. Truscott and P. E. Wellstead, "Bond graphs modeling for chassis control," in *IEE Colloq. Bond Graphs Control*, Apr. 1990, pp. 5/1–5/2.

[36] N. Coudert, G. Dauphin-Tanguy, and A. Rault, "Mechatronic design of an automatic gear box using bond graphs," in *Proc. Int. Conf. Systems, Man Cybern.*, Oct. 17–20, 1993, pp. 216–221.

[37] D. Jaume and J. Chantot, "A bond graph approach to the modeling of thermics problems under the hood," in *Proc. Int. Conf. Systems, Man Cybern.*, Oct. 17–20, 1993, pp. 228–233.

[38] G. A. Hubbard and K. Youcef-Toumi, "Modeling and simulation of a hybrid-electric vehicle drivetrain," in *Proc. 1997 Amer. Contr. Conf.*, Jun. 4–6, 1997, vol. 1, pp. 636–640.

[39] M. Filippa, C. Mi, J. Shen, and R. Stevenson, "Modeling of a hybrid electric vehicle test cell using bond graphs," *IEEE Trans. Vehic. Technol.*, vol. 54, no. 3, pp. 837–845, May 2005.

[40] S. Onoda and A. Emadi, "PSIM-based modeling of automotive power systems: Conventional, electric, and hybrid electric vehicles," *IEEE Trans. Vehic. Technol.*, vol. 53, no. 2, pp. 390–400, Mar. 2004.

[41] R. Juchem and B. Knorr, "Complete automotive electrical system design," in *Proc. 2003 Vehicular Technology Conf.*, Oct. 6–9, 2003, vol. 5, pp. 3262–3266.

[42] M. Ducusin, S. Gargies, B. Berhanu, and C. Mi, "Modeling of a series hybrid electric high mobility multipurpose wheeled vehicle," in *Proc. IEEE Vehicle Power and Propulsion Conf.*, Chicago, IL, Sep. 2005, pp. 561–566.

[43] M. Otter and H. Elmqvist. (2001, Jun.). "Modelica language, libraries, tools, workshop, and EU-project RealSim," in *The Modelica Organization*. [Online]. Available: http://www.modelica.org/documents/ModelicaOverview14.pdf

[44] L. Glielmo, O. R. Natale, and S. Santini, "Integrated simulations of vehicle dynamics and control tasks execution by Modelica," in *Proc. IEEE/ASME Int. Conf. Advanced Intelligent Mechatronics*, Jul. 20–24, 2003, vol. 1, pp. 395–400.

[45] [Online]. Available: http://www.synopsys.com/news/pubs/compiler/art2_saber-feb04.html

[46] L. Chu, Q. Wang, M. Liu, and J. Li, "Control algorithm development for parallel hybrid transit bus," in *Proc. IEEE Vehicle Power Propulsion Conf.*, Chicago, IL, Sep. 2005, pp. 196–200.

ABOUT THE AUTHORS

David Wenzhong Gao (Senior Member, IEEE) received the B.S. degree in aeronautical propulsion control engineering from Northwestern Polytechnic University, Xi'an, China, in 1988, and the M.S. and Ph.D. degrees in electrical and computer engineering specializing in electric power engineering from Georgia Institute of Technology, Atlanta, USA, in 1999 and 2002, respectively.

From 2002 to 2006, he has worked as an Assistant Research Professor in the University of South Carolina and Mississippi State University. Since 2006, he has worked as an Assistant Professor at Tennessee Tech University. His current research interests include hybrid electric propulsion systems, power system modeling and simulation, alternative power systems, renewable energy, and electric machinery and drive.

Chris Mi (Senior Member, IEEE) received the B.S.E.E. and M.S.E.E. degrees from Northwestern Polytechnical University, Xi'an, Shaanxi, China, and the Ph.D degree from the University of Toronto, Toronto, ON, Canada, all in electrical engineering.

He is an Assistant Professor at the University of Michigan, Dearborn, with teaching and research interests in the areas of power electronics, hybrid electric vehicles, electric machines and drives, renewable energy, and control. He joined General Electric Canada Inc., Peterborough, ON, as an Electrical Engineer in 2000, responsible for designing and developing large electric motors and generators. He was with the Rare-Earth Permanent Magnet Machine Institute of Northwestern Polytechnical University, Xi'an, Shaanxi, China, from 1988 to 1994. He joined Xi'an Petroleum Institute, Xi'an, Shaanxi, China, as an Associate Professor and Associate Chair of the Department of Automation in 1994. He was a Visiting Scientist at the University of Toronto from 1996 to 1997. He has recently developed a Power Electronics and Electrical Drives Laboratory at the University of Michigan. He has published more than 60 papers.

Dr. Mi is the recipient of many technical awards, including the Government Special Allowance (China) and Technical Innovation Award (China). He is the recipient of the Distinguished Teaching Award from the University of Michigan, in 2005. He is currently the Vice Chair of the IEEE Southeastern Michigan Section.

Ali Emadi (Senior Member, IEEE) received the B.S. and M.S. degrees in electrical engineering with highest distinction from Sharif University of Technology, Tehran, Iran. He received the Ph.D. degree in electrical engineering from Texas A&M University, College Station, where he was awarded the Electric Power and Power Electronics Institute fellowship for his graduate studies.

In 1997, he was a Lecturer at the Electrical Engineering Department of Sharif University of Technology. He joined the Electrical and Computer Engineering Department, Illinois Institute of Technology (IIT), in August 2000. He is the Director of the Grainger Power Electronics and Motor Drives Laboratories at IIT where he has established research and teaching laboratories as well as courses in power electronics, motor drives, and vehicular power systems. He is also the Co-founder and Co-director of IIT Consortium on Advanced Automotive Systems (ICAAS). His main research interests include modeling, analysis, design, and control of power electronic converters/systems and motor drives, integrated converters, vehicular power electronics, and electric and hybrid electric propulsion systems. He is the author of over 80 journal and conference papers as well as two books including *Vehicular Electric Power Systems: Land, Sea, Air, and Space Vehicles* (Marcel Dekker, 2003), and *Energy Efficient Electric Motors: Selection and Applications* (Marcel Dekker, 2004). He is also the Editor of the *Handbook of Automotive Power Electronics and Motor Drives* (Marcel Dekker, 2004).

Dr. Emadi is the recipient of the 2002 University Excellence in Teaching Award from IIT as well as Overall Excellence in Research Award from Office of the President, IIT, for mentoring undergraduate students. He directed a team of students to design and build a novel low-cost brushless DC motor drive for residential applications, which won the First Place Overall Award of the 2003 IEEE/DOE/DOD International Future Energy Challenge for Motor Competition. He is an Associate Editor of IEEE TRANSACTIONS ON POWER ELECTRONICS and a member of the editorial board of the *Journal of Electric Power Components and Systems*. He is a member of SAE. He is also listed in the *International Who's Who of Professionals* and *Who's Who in Engineering Academia*.